Omniphobic PVDF Nanofibrous Membrane for Superior Anti-wetting Performance in Direct Contact Membrane Distillation

Weihua Qing [a, b], Yifan Wu [a], Xianhui Li [a], Xiaonan Shi [a, b], Senlin Shao [a], Ying Mei [a], Wen Zhang [b], Chuyang Y. Tang [a,]*

a. Department of Civil Engineering, The University of Hong Kong, Pokfulam, Hong Kong 999077

b. John A. Reif, Jr. Department of Civil and Environmental Engineering, New Jersey Institute of Technology, Newark, NJ, 07102, United States

Abstract: Membrane wetting caused by low surface tension pollutants in feed solution has been a major challenge for membrane distillation (MD), and omniphobic membranes have been proposed as a promising solution to address this challenge due to their strong repellence towards liquids with a broad range of surface tensions. In this study, we report a nanoparticle-free strategy to fabricate omniphobic polyvinylidene fluoride (PVDF) nanofibrous membranes for robust MD desalination. A solvent-thermal induced roughening method was used to create multiscale hierarchical nanofin structures on electrospun PVDF nanofibers, followed by a polydopamine-anchored surface fluorination treatment to reduce the surface energy of the nanofibrous membrane. We show that the as-prepared membrane exhibited super repellence (>150°) to diverse liquids with surface tension ranging from 73 to 30 $mN \cdot m^{-1}$. Moreover, the omniphobic membrane maintained stable salt rejection and water flux in direct contact MD processes in the presence of sodium dodecyl sulfate surfactant (up to 0.4 mM) or mineral oil (up to 480 $mg \cdot L^{-1}$), demonstrating its promising potential in practical water reclamation from MD applications.

Keywords: Polyvinylidene fluoride (PVDF), membrane distillation, electrospinning, desalination, omniphobic membrane

1. Introduction

Membrane distillation (MD) is a promising thermally-driven desalination process for producing high-quality fresh water [1-3]. In MD, a hydrophobic porous membrane allows water vapor passage to the permeate stream under a vapor pressure gradient while preventing nonvolatile solute transportation [4]. MD is advantageous to distill water at lower pressures compared to reverse osmosis [5]. More attractively, it offers unique capability of harvesting waste or low-grade heat to desalinate high-salinity brines, and therefore has been regarded as a promising alternative water treatment process for areas where renewable or low-grade heat sources are readily available [6].

In principle, maintaining stable vapor/liquid interfaces at the hydrophobic membrane pores is critical to avoid failure of the MD desalination process. Unfortunately, conventional hydrophobic membranes show repellency only for water, but are highly vulnerable to low surface tension liquids [7]. In practical applications, a variety of low surface tension contaminants in the feed stream such as oils, surfactants, organic solvents often easily wet the hydrophobic pores and leads to direct feed passage to the permeate side, and thus significantly compromise the permeate water quality [8].

In recent years, omniphobic membranes, which display strong repellency (apparent contact angles of $>90°$) to both water and low-surface-tension liquids, has been suggested as a promising solution for sustainable MD process [9, 10]. Constructing omniphobic surfaces requires a smart combination of low surface energy surfaces and hierarchical reentrant microscopic structures [11, 12], and several successful designs of omniphobic membranes have been reported recently for robust MD treatment of low-surface-tension feed [13]. For example, the most common design involves depositing nanoparticles (e.g., SiO_2 [14], ZnO [15], TiO_2 [16]) to create reentrant micro-structures on a substrate membrane surfaces followed by surface fluorination to decease surface energy [14-19]. The resultant membranes showed both anti-water and anti-oil properties, and exhibited enhanced anti-wetting behavior for treating waters contaminated with

low-surface-tension liquids. However, this strategy is based on extrinsic additives deposition for reentrant structure construction, which often partially sacrifice the porosity of the pristine substrate and adversely affect the flux of the membrane [20]. In addition, the extrinsic additives also suffer from potential loss during long time operation, leading to limited durability of the membrane [21]. Several other omniphobic membrane designs have also been reported, such as electrospinning and CF_4 plasma treatment [22], layer-by-layer assembly followed by fluorination [23], long chain fluorododecyltrichlorosilane polymerization [24]. Nevertheless, these methods involve either sophisticated treatment procedures or harsh reaction/synthesis conditions, and thus potentially impede their practical applications in MD. Therefore, alternative techniques to prepare stable and high performance omniphobic membrane for robust MD application are desirable.

Recently, we developed a solvent-thermal induced roughening (STIR) method, based on a mechanism of anisotropic swelling and deformation, to create hierarchical nanofin structures on pristine polyvinylidene fluoride (PVDF) membranes [25]. The simplicity and versatility of this roughening method prompt us to further design robust omniphobic membranes for superior anti-wetting performances in MD. In the present study, we reported a combined STIR-fluorination strategy to prepare omniphobic PVDF nanofibrous membrane for treating surfactant and oil contaminated salty water in direct-contact membrane distillation (DCMD) process. As shown in **Figure 1**, a nanofibrous PVDF membrane was fabricated by electrospinning, followed by STIR treatment to constructing nanoscale reentrant structures on the pristine PVDF nanofibers. To further decreasing the surface energy, polydopamine (PDA) anchored surface fluorination was realized by self-assembling fluoroalkylsilane onto the roughed membranes. The physical and chemical properties of the membranes were systematically characterized by scanning electron microscopy (SEM), X-ray photoelectron spectroscopy (XPS), and Fourier transform infrared spectroscopy

(FTIR) analysis. Wettability of the membranes were further characterized to reveal the omniphobicity of the membranes. Finally, the anti-wetting performances of the membranes to sodium dodecyl sulfate (SDS) or mineral oil contaminated salty water were evaluated in DCMD experiments.

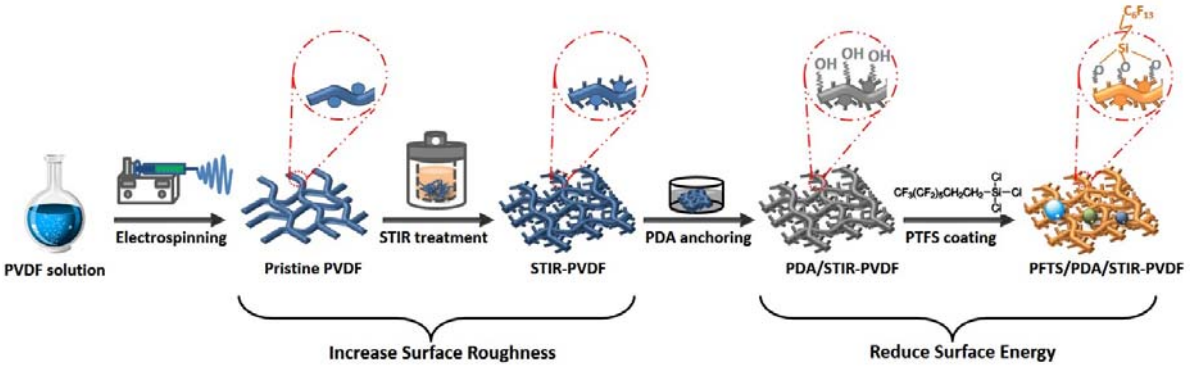

Figure 1. Preparation process for the omniphobic PVDF nanofibrous membrane

2. Methodology

2.1. Materials

PVDF beads (average molecular weight of ~180,000 Da), Tris (hydroxymethyl) aminomethane (≥99.0%, Tris-HCl), dopamine hydrochloride, N,N-Dimethylformamide (DMF, ReagentPlus, ≥99%) were all obtained from Sigma-Aldrich. n-pentanol, mineral oil, sodium chloride (NaCl), 1H,1H,2H,2H-perfluorooctyltrichlorosilane (PFTS) were all purchased by Dieckmann Co. Ltd. The anionic surfactant SDS was purchased from Uni-Chem Inc. Hydrogen chloride (HCl, 37 wt%) was received from VWR Chemicals Ltd.

2.2. Omniphobic PVDF nanofibrous membrane fabrication

2.2.1. Pristine PVDF nanofibrous membrane fabrication

The fabrication process was schematically illustrated in **Figure 1**. First, 5 g PVDF beads was completely dissolved in DMF at 60 °C to form a 25 wt. % PVDF solution. Afterwards, 15 mL of the

PVDF solution was loaded in the syringe of an electrospinning equipment to fabricate the pristine PVDF nanofibrous membrane using the following conditions: voltage of 24 kV, flow rate of 0.88 mL/h, collector diameter of 10 cm, collector rotating speed of 80 rpm, and spinneret to collector distance of 15 cm, spinneret size of 22 G. The electrospinning took approximately 6 hours and the as-prepared nanofibrous membrane was carefully torn off from the collector and placed in a drying oven at 60 °C overnight to remove any residual solvent before further treatment.

2.2.2. Omniphobic modification

The omniphobic modification of the pristine PVDF membrane involves two separated steps of multiscale roughness creation and surface fluorination (**Figure 1**). The multiscale roughness creation on pristine PVDF nanofibers was realized by a modified STIR methods: a piece of pristine PVDF membrane (9 cm × 16 cm) was carefully placed into a Teflon-lined autoclave. Then a solvent-thermal treatment solution containing 90 mL water, 90 mL HCl (37wt.%) and 3.24 mL n-pentanol was sequentially added into the autoclave before it was placed in an electric oven for hydrothermal treatment at 150 °C for 4 hours. Under a combined effect of solvent and heating, the shells of PVDF nanofibers were partially swelled and undergone more extensive thermal expansion than the non-swelled cores, resulting in the deformation of the shells relative to the cores to form surface roughness fins on the nanofibers [25]. The STIR treated membrane (denoted as STIR-PVDF) rinse thoroughly with excessive amount of ethanol and water multiple times to remove residual solutions and dried in the oven at 60 °C overnight.

The surface fluorination was achieved by PDA anchored fluoroalkylsilane coating. First, due to the highly nonreactive nature of the STIR-PVDF membrane, a mussel-inspired PDA layer was first coated to activate the membrane surface (denoted as PDA/STIR-PVDF): the membrane was immersed and mildly stirred in a 10 $mM \cdot L^{-1}$ Tris-HCl buffer solution (pH of 8.5) containing 2

115 mg·mL^{-1} dopamine hydrochloride for 1.5 hours, and then was taken out for rinse with excessive
116 amount of water in a ultrasonic bath to remove any loose PDA aggregates. The abundant hydroxyl
117 groups on the PDA layers can act as anchoring sites to react with fluoroalkylsilane in a chemical
118 vapor deposition process: the activated membrane was placed in a beaker with 100 μL PFTS, and
119 treated in a vacuum oven at 100 kPa and 100 °C for 60 min to complete the omniphobic
120 modification (denoted as PFTS/PDA/STIR-PVDF).

121 **2.3. Membrane characterization**

122 Membrane morphology was revealed by a Field Emission Gun SEM (FEG SEM, LEO-1530).
123 XPS was used to characterize the chemical composition variation by a spectrometer (Thermo Fisher
124 Scientific ESCALAB250. USA) with an X-ray source of monochromic Al Kα 150 W. FTIR
125 analysis was performed to investigate the surface functional groups of the membranes by a Nicolet
126 8700 (Thermo Scientific). Contact angle measurements were conducted by Attention Theta system
127 from Biolin Scientific. For each measurement, one testing droplet (~ 6 μL) was slowly released on
128 flat sample surface, and a stabilization time of 10 s was allowed before contact angle determination.
129 Dynamic droplet contacting process was also recorded by the platform to characterize the droplet
130 adhesion behaviors on the membranes. Sliding angles were determined by a manual goniometer. A
131 digital calipers was used to determine the average membrane thickness from five different locations.
132 Membrane porosity and liquid entry pressure (LEP) were determined by gravimetric method and a
133 capillary flow porometer (POROLUX™ 1000, Germany), respectively as described in our previous
134 study [25].

135

136 **2.4. DCMD experiments**

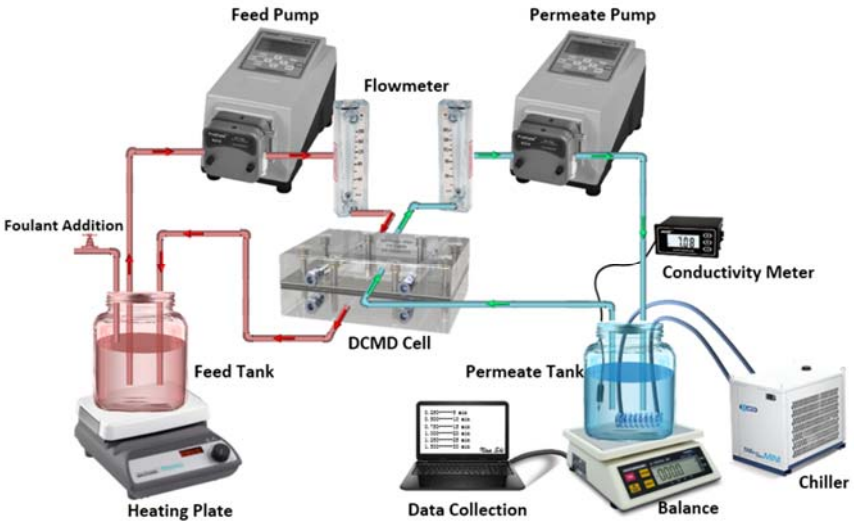

Figure 2. Schematic illustration of the DCMD apparatus.

The anti-wetting performances of the membranes were evaluated in a custom-made DCMD apparatus (**Figure 2**). In a typical experiment, 1.5 L synthetic seawater of 3.5 wt. % NaCl was heated to 60 ^{o}C (IKA heating plate, RCT basic, Germany), and circulated through the feed side of the membrane module (effective membrane area of 9 cm^2) with a flow rate of 440 mL/min (Longer peristaltic pump, BT600-2J, China). Meantime, cold water maintained at 20 ^{o}C (CNSHP chiller, DC0605, China) was counter-currently circulated through the permeate side of the module with the same flow rate. The flat sheet nanofibrous membranes were directly mounted between the feed and permeate side of the module without using supporting materials. The cold water tank (permeate tank) was placed on a weighing scale (OHAUS scale, Adventurer Pro AV8101, USA), and its weight increase was continuously recorded for flux determination. The conductivity of the permeate was monitored (Sinomeasure conductivity meter, SIN-TDS310, China) for rejection calculation. The system was pre-stabilized for 2 hours, after which contaminants of SDS or mineral oil emulsion (10 mL mineral oil and 1 mL Tween 80 stabilized in 1 L water) were injected into the feed tank progressively (every one hour) to reduce the feed surface tension. To maintain the foulant concentration variation the feed was replenished with Milli-Q water every 2 hours.

3. Results and discussion

3.1. Membrane morphology

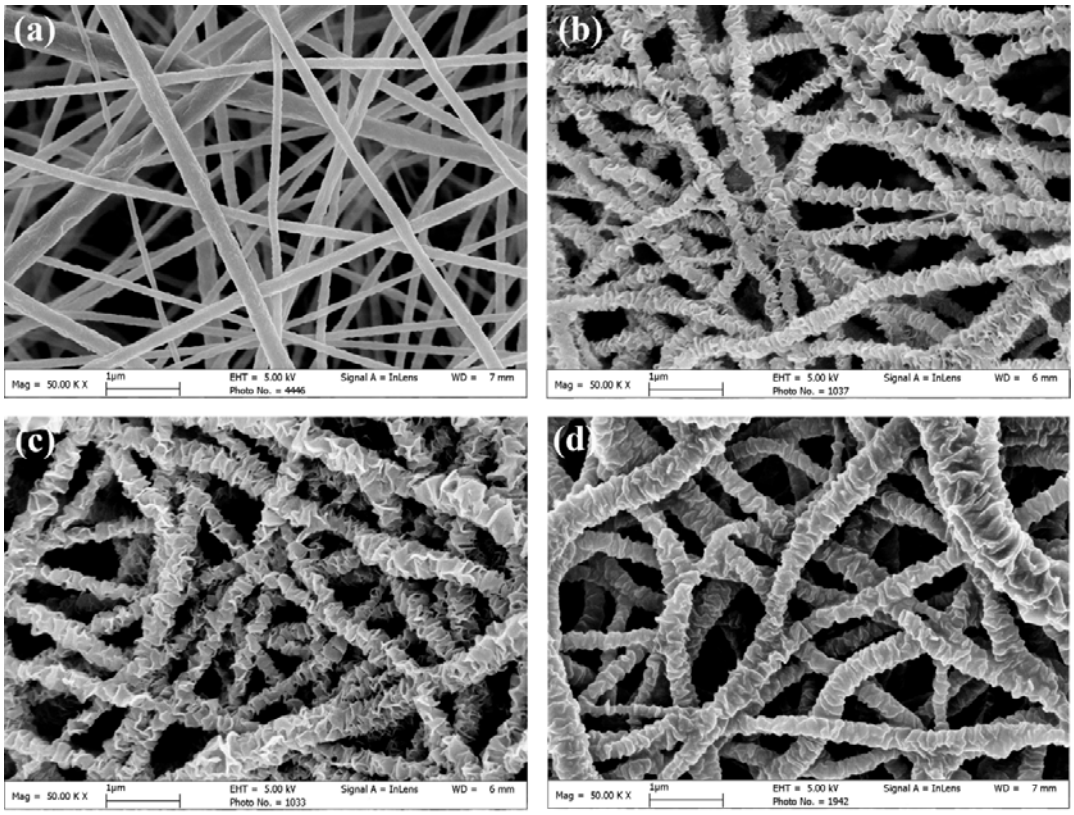

Figure 3. SEM images showing the top view of (a) the pristine PVDF membrane, (b) STIR-treated membrane, (c) PDA activated PDA/STIR-PVDF membrane, and (d) fluorinated PFTS/PDA/STIR-PVDF membrane.

Table 1. Some membrane characteristics before and after omniphobic modification

	Mean fiber diameter (nm)	Porosity (%)	Max pore size (nm)	Mean pore size (nm)	Thickness (mm)
Pristine PVDF membrane [a]	186±49	89±1.3	1054±119	909±5	0.18±0.02
PFTS/PDA/STIR-PVDF membrane	309±79	82±1.2	616±63	358±35	0.19±0.02

[a] The data of max pore size and mean pore size of the pristine membrane have been disclosed in our previous report [25].

The surface morphology variations of the membranes during the omniphobic modification process was revealed by SEM analysis (**Figure 3**). The pristine PVDF nanofibrous membrane had a typical electrospun nanofibrous morphology, with smooth nanofibers with a mean diameter of 186 nm randomly interwoven to form a 3D porous network (**Figure 3a**). Remarkably, the STIR-treated

membrane was significantly roughened by the coverage of enormous nanofin structures on the nanofibers (**Figure 3b**), which was created by an anisotropic swelling and deformation roughening mechanism [25]: the pristine nanofiber was partially swelled by the hydrothermal treatment solution to form a swelled-soft-shell/non-swelled-hard-core transitional structure, followed by the consequent deformation of the swelled soft shell (driven the mismatched internal stress) to create nanofin structure on the non-swelled hard core. After PDA surface activation (**Figure 3c**) and PFTS surface fluorination (**Figure 3d**), the morphologies of both resultant membranes showed no obvious changes when compared to the STIR-PVDF membrane. Some fundamental membrane characteristics were presented in **Table 1**. After omniphobic modification, the average PVDF nanofiber diameters increased from 186±49 to 309±79 nm while the mean pore sizes decreased from 909±5 to 358±35 nm, which can be ascribed from the combined effects of fiber swelling and roughness creation [25]. However, the porosity was only slightly affected due to the multiscale hierarchical structures of the treated membrane.

3.2. Membrane surface chemical compositions

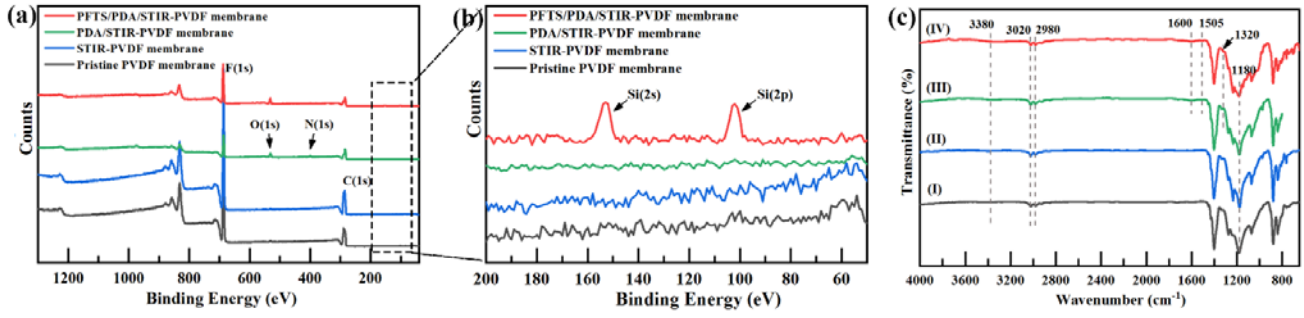

Figure 4. Surface chemical composition characterization by (a) (b) XPS survey spectra (Note that spectra of pristine PVDF membrane has been disclosed in our previous report [21]), and (c) FTIR-ATR spectra of different membranes: (I) pristine PVDF, (II) STIR-PVDF, (III) PDA/STIR-PVDF, and (IV) PFTS/PDA/STIR-PVDF membranes.

The surface chemical components were determined by XPS (**Figure 4a,b**). The STIR-PVDF membrane only had carbon and fluorine element detected as the pristine PVDF membrane, due to

189 the fact that the STIR method only induces roughness creation instead of chemical modification
190 [25]. Oxygen and nitrogen elements were detected on the PDA/STIR-PVDF membrane, which can
191 be attributed to the PDA surface coating. Furthermore, additional silicon element with peaks of
192 Si(2s) and Si(2p) were only found on the PFTS/PDA/STIR-PVDF membrane, indicating successful
193 fluorination of the membrane.

194 The surface functional groups of the membranes were further investigated by FTIR-ATR
195 analysis (**Figure 4c**). Absorption band at 1180 cm^{-1} is associated with $–CF_2$ [26], and the absorption
196 bands at 3020 and 2980 cm^{-1} are associated with asymmetric and symmetric vibration of $–CH_2$,
197 respectively [27]. PDA is the most notable coating agent in recent years, which offers attractive
198 mussel-like adhesive properties and can firmly attach to different substrate with robust binding
199 strength [28]. It can be seen that new absorption signals at 1600 cm^{-1} and 1505 cm^{-1} appears on the
200 PDA/STIR-PVDF membrane, which can be assigned to the C=C resonance vibrations in the
201 aromatic ring and N–H bending vibrations, respectively [29]. In addition, a wide absorption signal
202 between 3500 and 3100 cm^{-1} was also detected which can be assigned to N–H and O–H stretching
203 vibrations [30]. These observations confirmed the PDA activation on the membranes. After surface
204 fluorination treatment, new adsorption band at 1320 cm^{-1} which corresponds to the stretching
205 vibration of $–CF_3$ [31] confirms the successful PFTS grafting. PFTS has a trichlorosilane based
206 “head group” which can readily reacts with the hydroxyl groups on the PDA activation layer to
207 form very stable R-Si-O-substrate covalent bond [32].

208 **3.3. Membrane wettability**

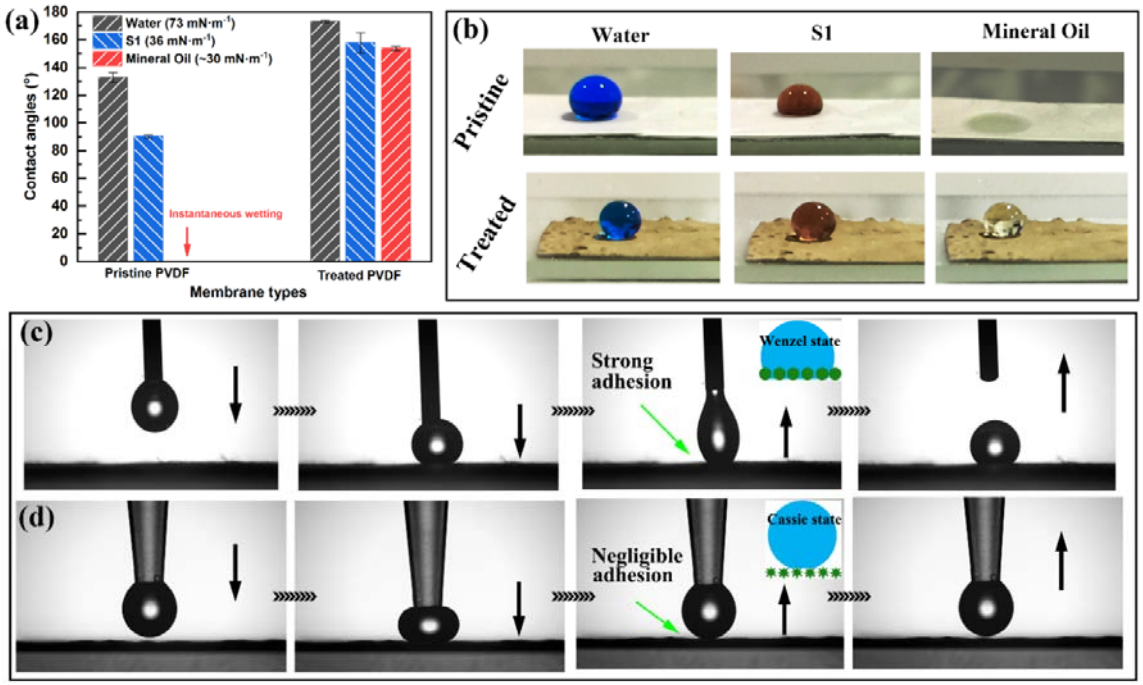

Figure 5. Wettability characterization results of (a) contact angle measurements, (b) photos of different liquid droplets, noting that liquid S1 is 3.5 wt.% NaCl solution with 0.25 mM SDS, and (c) water dynamic contacting behavior measurements on pristine PVDF membrane and (d) PFTS/PDA/STIR-PVDF membrane.

The wettability of the pristine PVDF and treated PFTS/PDA/STIR-PVDF nanofibrous membranes were characterized by contact angle and water dynamic contacting behavior measurements. **Figure 5a** present the contact angle results of different liquid drops on the two membranes, including water, surfactant contaminated saline water, and mineral oil with surface tensions of 73, 36, and 30 $mN \cdot m^{-1}$, respectively. The pristine membrane exhibited fair hydrophobicity to pure water and surfactant contaminated saline water, but it was instantaneously wetted by mineral oil (**Figure 5b**). In contrast, the PFTS/PDA/STIR-PVDF membrane displayed excellent repellence to all the tested liquids with the contact angles all higher than 150°, showing superomniphobic property of the treated membrane.

Water dynamic contacting behaviors on pristine and treated membrane are presented in **Figure 5c, d**, where a water droplet slowly touched a membrane surface and was then lifted away. Clearly, when the droplet was detaching the pristine PVDF membrane surface, it was dramatically stretched

before it was eventually captured on the membrane surface (**Figure 5c**). This sticky phenomenon indicated strong adhesion between the water droplet and the pristine membrane, implying a Wenzel's wetting state where the droplet penetrate and fill the air pockets of the pristine PVDF membranes (see insert in **Figure 5c**) and results in high adhesive forces between the water and the substrate [33]. In contrast, the shape of the water droplet showed almost no elongation when it was lifted away from the treated PFTS/PDA/STIR-PVDF membrane (**Figure 5d**), showing a negligible interaction between the water and treated membrane. This suggested a Cassie's wetting state that the water droplet cannot enter the interstices between the treated nanofibers and had minimum liquid/nanofiber contacting interfaces (see insert in **Figure 5d**) [34], which significantly reduce the water affinity of the PFTS/PDA/STIR-PVDF membrane.

LEP, defined as the critical pressure at which liquid starts to penetrate inside the membrane pores, is an important parameter to evaluate how wettable a hydrophobic membrane is toward different liquid solutions. The LEP of the pristine PVDF membrane was 83±3 kPa [25], while that of treated PFTS/PDA/STIR-PVDF membrane was greatly improved to 216±29 kPa. The enhancement in LEP can be attributed to the reduced mean pore size and improved hydrophobicity of the treated membrane, implying better anti-wetting property and operational stability.

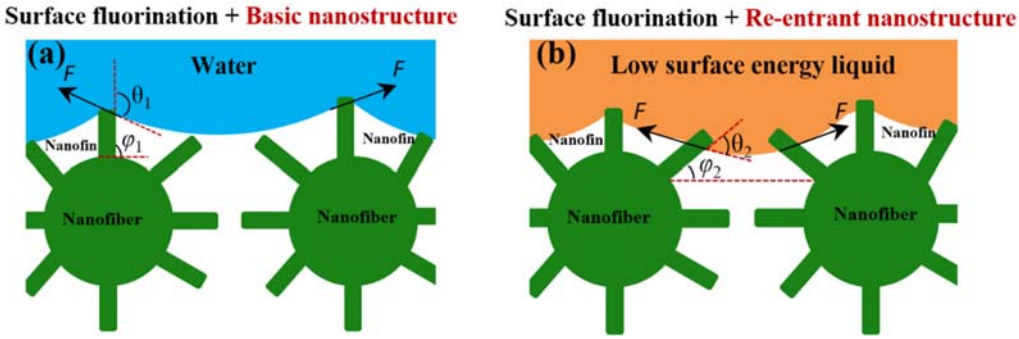

Figure 6. Possible suspension behavior of (a) water and (b) low surface energy liquid on the PFTS/PDA/STIR-PVDF membrane. θ is intrinsic contact angle, and φ is local texture angle.

To better understand the anti-wetting mechanism of the omniphobic membrane, a conceptual

model to illustrate the suspension behaviors of both water and low surface energy liquid on the liquid-air interface of a PFTS/PDA/STIR-PVDF membrane (**Figure 6**). When a water droplet was deposited on the membrane surface, the intrinsic water contact angle on the membrane θ_1 was greater than 90° due to surface fluorination (**Figure 6a**). In this case of $\theta_1 > \varphi_1 \geq 90°$, the water droplet cannot further enter into the interstices among the nanofibers due to upward net traction [9, 35]. As for low surface energy liquid depositing on the PFTS/PDA/STIR-PVDF membrane, though the intrinsic contact angle θ_2 was smaller than 90° [17], it was still larger than the local texture angle φ_2 due to the nanofins create reentrant nanostructure in the membranes (**Figure 6b**). In this case, the low surface energy liquid may invade the basic nanostructure, but cannot enter further into the reentrant nanostructure due to $90° > \theta_2 > \varphi_2 \geq 0°$ [35]. Therefore, the resultant upward net traction realized wetting resistance of the membrane toward low surface energy liquid such as surfactant or oils.

3.4. Anti-wetting performances in DCMD

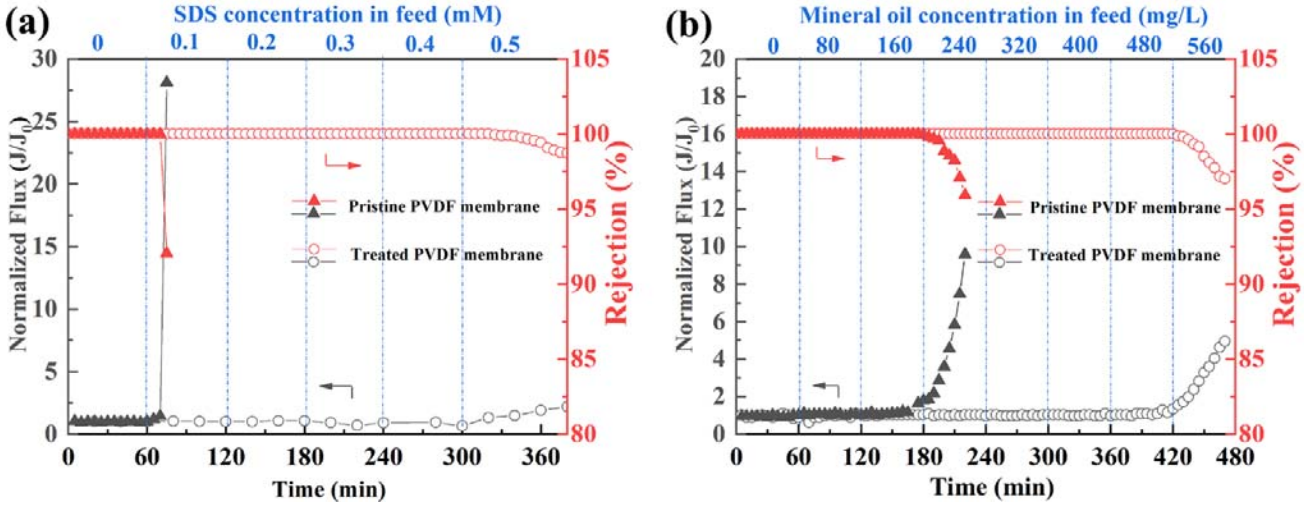

Figure 7. Normalized flux and salt rejection of pristine PVDF membrane and omniphobic PFTS/PDA/STIR-PVDF membrane in DCMD desalination with progressive contaminants addition of (a) SDS (the initial fluxes of the pristine and treated membranes were 26 and 17 Kg • $m^{-2} \cdot h^{-1}$, respectively), or (b) mineral oil-in-water emulsion (the initial fluxes of the pristine and treated membranes were 25 and 20 $Kg \cdot m^{-2} \cdot h^{-1}$, respectively).

Table 2. Comparison of anti-wetting and antifouling performances of omniphobic membranes for DCMD application

Membrane substrate	Modification method	Feed composition	Feed/permeate inlet temperatures (°C)	Initial flux ($Kg \cdot m^{-2} \cdot h^{-1}$)	Surfactant SDS tolerance (mM)	Organic pollutant tolerance	Publication year and Ref.
PVDF microfiltration membrane	Silica deposition followed by FDTS surface coating	1 M NaCl aqueous solution	60/20	13.6	0.2	80 mg/L mineral oil-in-water emulsion	2016, [18]
PVDF microfiltration membrane	Flurinated ZnO/PVDF-HFP nanoparticles deposition	3.5 wt% NaCl solution	60/20	~24	0.4	0.015 v/v saline oil solution	2019, [36]
PVDF microfiltration membrane	waterborne solution coating containing fluorocarbon surfactant, fluorinated alkyl silane, and silicon dioxide nanoparticles	3.5 wt% NaCl solution	70/20	27	0.4	0.01 % v/v mineral oil or kerosene	2019, [37]
PVDF-HFP nanofibrous membrane	TiO2 nanostructures deposition followed by PFTS coating	3.5 wt% NaCl solution	60/20	13.8~20.5	0.4	320 mg/L mineral oil-in-water emulsion	2020, [16]
PVDF nanofibrous membrane	Solvent-thermal induced roughening followed by PFTS coating	3.5 wt% NaCl solution	60/20	17~20	0.5	480 mg/L mineral oil-in-water emulsion	This work

The anti-wetting performances of the pristine and treated PVDF nanofibrous membranes in DCMD were evaluated by progressively adding contaminants, i.e., surfactant SDS or mineral oil emulsion, into the feed stream every hour to challenge the membranes. Both membranes showed stable flux and rejection when the contaminants were absent. However, when merely 0.1 mM SDS was added, the pristine PVDF membrane immediately failed with dramatic flux surge and rejection decline, implying the pristine membrane pores were severely wetted after the SDS dosage (**Figure 7a**). Remarkably, the omniphobic PFTS/PDA/STIR-PVDF membrane maintained stable flux and complete salt rejection (no conductivity increase observed at the permeate) for SDS concentration up to 0.4 mM. The desalination performance only started to compromise after 0.5 mM SDS dosage, but the membrane still maintained decent salt rejection of 99.4 %, suggesting that only limited membrane pores were wetted at this high surfactant concentration (**Figure 7a**). These observations confirmed the excellent wetting resistance for surfactant-contaminated feedwater of the omniphobic membrane.

Mineral oil emulsion was progressively added into the feedwater to challenge the pristine and treated membranes in DCMD (**Figure 7b**). Similar to the desalination behaviors with surfactant addition, the pristine membrane started to fail with gradual flux rise and rejection decline after the oil concentration reached 240 mg/L, whereas, the treated PFTS/PDA/STIR-PVDF membrane still offered stable flux together with complete salt rejection when doubling the oil concentration to 480 $mg \cdot L^{-1}$. This remarkable contrast further highlighted the superior anti-wetting ability of the treated membrane, which can be ascribed from the low affinity of the omniphobic membrane surface to low surface energy liquids. Moreover, **Table 2** summarized the anti-wetting performances of previously reported membranes towards both surfactant and oils in DCMD application. Compared to the existing literature values, our omniphobic PFTS/PDA/STIR-PVDF membrane exhibited

higher SDS and oil tolerances, suggesting a promising potential for practical DCMD applications.

4. Conclusions

In summary, we developed an omniphobic PVDF nanofibrous membrane by a STIR-fluorination combined strategy for superior anti-wetting performance in DCMD application. We showed that the STIR treatment induced hierarchical PVDF nanofin structures on the pristine PVDF nanofiber, while the PDA anchored PFTS coating fluorinated the roughened surface. The synergy of the multiscale surface roughness and low surface energy enabled superomniphobic property for the PVDF nanofibrous membrane, with water contact angle of 173.2 ° and mineral oil contact angle of 153.8 °. We further demonstrated that the omniphobic membrane exhibited robust anti-wetting ability towards surfactant (SDS tolerance up to 0.4 mM) or oil (mineral oil tolerance up to 480 $mg \cdot L^{-1}$) contaminated seawater in DCMD process. Our method provided a nanoparticle-free strategy to prepare robust omniphobic membranes for potential practical MD desalination applications.

Acknowledgement

The authors appreciate the financial support from a Joint Research Scheme between Research Grants Council of Hong Kong and National Natural Science Foundation of China (No. N_HKU706/16).

References:

[1] A. Deshmukh, C. Boo, V. Karanikola, S. Lin, A.P. Straub, T. Tong, D.M. Warsinger, M. Elimelech, Membrane distillation at the water-energy nexus: limits, opportunities, and challenges, Energy & Environmental Science, 11 (2018) 1177-1196.

[2] D. Rice, S.J. Ghadimi, A.C. Barrios, S. Henry, W.S. Walker, Q. Li, F. Perreault, Scaling Resistance in Nanophotonics-Enabled Solar Membrane Distillation, Environmental Science & Technology, (2020).

[3] W. Jia, J.A. Kharraz, P.J. Choi, J. Guo, B.J. Deka, A.K. An, Superhydrophobic membrane by hierarchically

structured PDMS-POSS electrospray coating with cauliflower-shaped beads for enhanced MD performance, Journal of Membrane Science, 597 (2020) 117638.
[4] A. Alkhudhiri, N. Darwish, N. Hilal, Membrane distillation: A comprehensive review, Desalination, 287 (2012) 2-18.
[5] P.S. Goh, T. Matsuura, A.F. Ismail, N. Hilal, Recent trends in membranes and membrane processes for desalination, Desalination, 391 (2016) 43-60.
[6] B. Ashoor, S. Mansour, A. Giwa, V. Dufour, S. Hasan, Principles and applications of direct contact membrane distillation (DCMD): A comprehensive review, Desalination, 398 (2016) 222-246.
[7] L.D. Tijing, Y.C. Woo, J.-S. Choi, S. Lee, S.-H. Kim, H.K. Shon, Fouling and its control in membrane distillation—A review, Journal of Membrane Science, 475 (2015) 215-244.
[8] M. Yao, L.D. Tijing, G. Naidu, S.-H. Kim, H. Matsuyama, A.G. Fane, H.K. Shon, A review of membrane wettability for the treatment of saline water deploying membrane distillation, Desalination, 479 (2020) 114312.
[9] K.J. Lu, Y. Chen, T.-S. Chung, Design of omniphobic interfaces for membrane distillation–A review, Water Research, (2019).
[10] N.G.P. Chew, S. Zhao, R. Wang, Recent advances in membrane development for treating surfactant- and oil-containing feed streams via membrane distillation, Advances in Colloid and Interface Science, 273 (2019) 102022.
[11] K.J. Lu, J. Zuo, J. Chang, H.N. Kuan, T.-S. Chung, Omniphobic Hollow-Fiber Membranes for Vacuum Membrane Distillation, Environmental Science & Technology, 52 (2018) 4472-4480.
[12] J.A. Kharraz, M.U. Farid, N.K. Khanzada, B.J. Deka, H.A. Arafat, A.K. An, Macro-corrugated and nano-patterned hierarchically structured superomniphobic membrane for treatment of low surface tension oily wastewater by membrane distillation, Water Research, (2020) 115600.
[13] W. Wang, X. Du, H. Vahabi, S. Zhao, Y. Yin, A.K. Kota, T. Tong, Trade-off in membrane distillation with monolithic omniphobic membranes, Nature communications, 10 (2019) 1-9.
[14] R. Zheng, Y. Chen, J. Wang, J. Song, X.-M. Li, T. He, Preparation of omniphobic PVDF membrane with hierarchical structure for treating saline oily wastewater using direct contact membrane distillation, Journal of Membrane Science, 555 (2018) 197-205.
[15] L.-H. Chen, Y.-R. Chen, A. Huang, C.-H. Chen, D.-Y. Su, C.-C. Hsu, F.-Y. Tsai, K.-L. Tung, Nanostructure depositions on alumina hollow fiber membranes for enhanced wetting resistance during membrane distillation, Journal of Membrane Science, 564 (2018) 227-236.
[16] X. Li, W. Qing, Y. Wu, S. Shao, L.E. Peng, Y. Yang, P. Wang, F. Liu, C.Y. Tang, Omniphobic Nanofibrous Membrane with Pine-Needle-Like Hierarchical Nanostructures: Toward Enhanced Performance for Membrane Distillation, ACS Applied Materials & Interfaces, 11 (2019) 47963-47971.
[17] C. Boo, J. Lee, M. Elimelech, Engineering Surface Energy and Nanostructure of Microporous Films for Expanded Membrane Distillation Applications, Environmental Science & Technology, 50 (2016) 8112-8119.
[18] C. Boo, J. Lee, M. Elimelech, Omniphobic polyvinylidene fluoride (PVDF) membrane for desalination of shale gas produced water by membrane distillation, Environmental science & technology, 50 (2016) 12275-12282.
[19] S. Lin, S. Nejati, C. Boo, Y. Hu, C.O. Osuji, M. Elimelech, Omniphobic membrane for robust membrane distillation, Environmental Science & Technology Letters, 1 (2014) 443-447.
[20] L.N. Nthunya, L. Gutierrez, S. Derese, E.N. Nxumalo, A.R. Verliefde, B.B. Mamba, S.D. Mhlanga, A review of nanoparticle‐enhanced membrane distillation membranes: membrane synthesis and applications in water treatment, Journal of Chemical Technology & Biotechnology, 94 (2019) 2757-2771.
[21] W. Qing, J. Wang, X. Ma, Z. Yao, Y. Feng, X. Shi, F. Liu, P. Wang, C.Y. Tang, One-step tailoring surface roughness and surface chemistry to prepare superhydrophobic polyvinylidene fluoride (PVDF) membranes for enhanced membrane distillation performances, Journal of Colloid and Interface Science, 553 (2019) 99-107.
[22] Y. Chul Woo, Y. Chen, L.D. Tijing, S. Phuntsho, T. He, J.-S. Choi, S.-H. Kim, H. Kyong Shon, CF4

plasma-modified omniphobic electrospun nanofiber membrane for produced water brine treatment by membrane distillation, Journal of Membrane Science, 529 (2017) 234-242.
[23] Y.C. Woo, Y. Kim, M. Yao, L.D. Tijing, J.-S. Choi, S. Lee, S.-H. Kim, H.K. Shon, Hierarchical Composite Membranes with Robust Omniphobic Surface Using Layer-By-Layer Assembly Technique, Environmental Science & Technology, 52 (2018) 2186-2196.
[24] L. Deng, H. Ye, X. Li, P. Li, J. Zhang, X. Wang, M. Zhu, B.S. Hsiao, Self-roughened omniphobic coatings on nanofibrous membrane for membrane distillation, Separation and Purification Technology, 206 (2018) 14-25.
[25] W. Qing, X. Shi, W. Zhang, J. Wang, Y. Wu, P. Wang, C.Y. Tang, Solvent-thermal induced roughening: A novel and versatile method to prepare superhydrophobic membranes, Journal of Membrane Science, 564 (2018) 465-472.
[26] W. Qing, X. Shi, Y. Deng, W. Zhang, J. Wang, C.Y. Tang, Robust superhydrophobic-superoleophilic polytetrafluoroethylene nanofibrous membrane for oil/water separation, Journal of Membrane Science, 540 (2017) 354-361.
[27] J. Oku, R.J. Chan, H. Hall, O. Hughes, Synthesis of a poly (vinylidene fluoride) macromonomer, Polymer Bulletin, 16 (1986) 481-485.
[28] Q. Huang, J. Chen, M. Liu, H. Huang, X. Zhang, Y. Wei, Polydopamine-based functional materials and their applications in energy, environmental, and catalytic fields: State-of-the-art review, Chemical Engineering Journal, 387 (2020) 124019.
[29] L. Shao, Z.X. Wang, Y.L. Zhang, Z.X. Jiang, Y.Y. Liu, A facile strategy to enhance PVDF ultrafiltration membrane performance via self-polymerized polydopamine followed by hydrolysis of ammonium fluotitanate, Journal of Membrane Science, 461 (2014) 10-21.
[30] J. Jiang, L. Zhu, L. Zhu, B. Zhu, Y. Xu, Surface Characteristics of a Self-Polymerized Dopamine Coating Deposited on Hydrophobic Polymer Films, Langmuir, 27 (2011) 14180-14187.
[31] H. Wang, Z. Liu, X. Zhang, C. Lv, R. Yuan, Y. Zhu, L. Mu, J. Zhu, Durable Self-Healing Superhydrophobic Coating with Biomimic “Chloroplast” Analogous Structure, Advanced Materials Interfaces, 3 (2016) 1600040.
[32] J. Bong, J. Lee, J. Lee, Y.G. Ha, S. Ju, Development of omniphobic behavior in molecular self‐assembled monolayer‐coated nanowire forests, Journal of Biomedical Materials Research Part B: Applied Biomaterials, 105 (2017) 204-210.
[33] L. Feng, Y. Zhang, J. Xi, Y. Zhu, N. Wang, F. Xia, L. Jiang, Petal Effect: A Superhydrophobic State with High Adhesive Force, Langmuir, 24 (2008) 4114-4119.
[34] M. Nosonovsky, B. Bhushan, Why re-entrant surface topography is needed for robust oleophobicity, Philosophical Transactions of the Royal Society A: Mathematical, Physical and Engineering Sciences, 374 (2016) 20160185.
[35] T. Liu, C.-J. Kim, Turning a surface superrepellent even to completely wetting liquids, Science, 346 (2014) 1096-1100.
[36] B.J. Deka, J. Guo, N.K. Khanzada, A.K. An, Omniphobic re-entrant PVDF membrane with ZnO nanoparticles composite for desalination of low surface tension oily seawater, Water Research, 165 (2019) 114982.
[37] X. Li, H. Shan, M. Cao, B. Li, Facile fabrication of omniphobic PVDF composite membrane via a waterborne coating for anti-wetting and anti-fouling membrane distillation, Journal of Membrane Science, 589 (2019) 117262.